NeuroImage: Clinical 22 (2019) 101760

Contents lists available at ScienceDirect

NeuroImage: Clinical

journal homepage: www.elsevier.com/locate/ynicl

Attenuated mismatch negativity in patients with first-episode antipsychotic-naive schizophrenia using a source-resolved method

Randau M.[a], Oranje B.[a,c,d,*], Miyakoshi M.[e], Makeig S.[e], Fagerlund B.[a,b], Glenthøj B.[a,d], Bak N.[a]

[a] Centre for Neuropsychiatric Schizophrenia Research and Centre for Clinical Intervention and Neuropsychiatric Schizophrenia Research, Mental Health Centre Glostrup, University of Copenhagen, Denmark
[b] Department of Psychology, University of Copenhagen, Denmark
[c] Department of Psychiatry, Brain Center Rudolf Magnus, University Medical Center Utrecht, Utrecht, the Netherlands
[d] Faculty of Health and Medical Sciences, Department of Clinical Medicine, University of Copenhagen, Copenhagen, Denmark
[e] Swartz Center for Computational Neuroscience, Institute for Neural Computation, University of California San Diego, La Jolla, CA, USA.

ARTICLE INFO

Keywords:
Mismatch negativity
Schizophrenia
First episode
EEG
ICA

ABSTRACT

Background: Mismatch negativity (MMN) is a measure of pre-attentive auditory information processing related to change detection. Traditional scalp-level EEG methods consistently find attenuated MMN in patients with chronic but not first-episode schizophrenia. In the current paper, we use a source-resolved method to assess MMN and hypothesize that more subtle changes can be identified with this analysis method.

Method: Fifty-six first-episode antipsychotic-naïve schizophrenia (FEANS) patients (31 males, 25 females, mean age 24.6) and 64 matched controls (37 males, 27 females, mean age 24.8) were assessed for duration-, frequency- and combined-type MMN and P3a as well as 4 clinical, 3 cognitive and 3 psychopathological measures. To evaluate and correlate MMN at source-level, independent component analysis (ICA) was applied to the continuous EEG data to derive equivalent current dipoles which were clustered into 19 clusters based on cortical location.

Results: No scalp channel group MMN or P3a amplitude differences were found. Of the localized clusters, several were in or near brain areas previously suggested to be involved in the MMN response, including frontal and anterior cingulate cortices and superior temporal and inferior frontal gyri. For duration deviants, MMN was attenuated at the right superior temporal gyrus in patients compared to healthy controls ($p = 0.01$), as was P3a at the superior frontal cortex ($p = 0.01$). No individual patient correlations with clinical, cognitive, or psychopathological measures survived correction for multiple comparisons.

Conclusion: Attenuated source-localized MMN and P3a peak contributions can be identified in FEANS patients using a method based on independent component analysis (ICA). This indicates that deficits in pre-attentive auditory information processing are present at this early stage of schizophrenia and are not the result of disease chronicity or medication. This is to our knowledge the first study on FEANS patients using this more detailed method.

1. Introduction

Schizophrenia is a mental illness characterized by positive symptoms (*e.g.*, auditory hallucinations, delusions), negative symptoms (*e.g.*, flattening of affects, social isolation), and cognitive deficits (*e.g.* deficits in attention and memory). The underlying causes of schizophrenia are of both genetic and environmental origin, with current models involving disturbances in early information processing, dysregulation of dopamine, abnormal *N*-methyl-D-aspartate (NMDA) receptor functioning and disruptions of connectivity (Baumeister and Francis, 2002; Friston et al., 2016; Javitt et al., 2012; Olney et al., 1999).

One measure thought to index early information processing is mismatch negativity (MMN), a pre-attentive mismatch between covertly expected and received auditory input. MMN can be obtained using an unattended auditory oddball paradigm in which deviant tones are interspersed among common standard tones, commonly differing from them either in terms of duration, frequency or intensity. MMN can be recorded using both electroencephalography (EEG) and magnetoencephalography and is identified in the event-related potential (ERP) difference between ERPs time locked to onsets of deviant and standard

* Corresponding author.
E-mail address: b.oranje@cnsr.dk (B. Oranje).

https://doi.org/10.1016/j.nicl.2019.101760
Received 19 September 2018; Received in revised form 6 February 2019; Accepted 10 March 2019
Available online 12 March 2019

tones, respectively. In the traditional method this response difference is measured at one (usually frontocentral Fz or FCz) or across a few scalp channels. MMN is a frontocentral scalp negative deflection peaking between 100 and 250 ms post-stimulus that is polarity-reversed (positive-going) on the scalp at electrode channels near the mastoids. Since its first description by Näätänen (1978), the MMN size and latency has been used extensively to study brain auditory processing mechanisms (reviewed in Näätänen et al., 2007). MMN is usually followed by a peak sometimes referred to as P3a, a midfrontal positive peak between 250 and 300 ms thought to index involuntary attentional reorientation towards the deviant stimulus (Escera et al., 1998).

Several brain regions have been implicated in the generation of MMN, including the auditory cortex, superior temporal gyrus, inferior frontal gyrus, frontal cortex, anterior cingulate cortex and insula (Gaebler et al., 2015; Giard et al., 1990; Waberski et al., 2001). Rissling et al. (2014, discussed below) reported contributions from at least 6 cortical areas to the MMN complex recorded from the scalp. Furthermore, there is evidence that the supratemporal sources are active ~10–20 ms earlier than the frontal sources (Fulham et al., 2014; Kim et al., 2016; Rinne et al., 2000). For frequency deviants, some studies have described an earlier component at 90–120 ms post-stimulus, thought to originate in the superior temporal gyrus, while the following MMN originates in the inferior frontal gyrus (Doeller et al., 2003; Opitz et al., 2002).

MMN has been described in terms of predictive coding (Garrido et al., 2007a; Wacongne et al., 2012), and this idea is supported by data (Powers et al., 2017). In the predictive coding theory, the brain is organized hierarchically, with higher-order stimulus event processing levels sending predictions to lower levels. When the presentation of a new stimulus does not match its prediction, a MMN response (indexing prediction error) is generated at the lowest processing level and sent upwards in the hierarchy, and this mismatch signalling is involved in updating the predictive model. The auditory cortex, superior temporal gyrus and inferior frontal gyrus are regarded as input regions for the predictive coding model of the MMN response (Garrido et al., 2007b; Lieder et al., 2013; Wacongne et al., 2012; Winkler, 2007).

MMN was first linked to schizophrenia in 1991 when Shelley et al. found that chronic schizophrenia patients had attenuated duration deviant MMN (Shelley et al., 1991). Today, attenuated frequency- and duration deviant MMN is consistently found in chronic schizophrenia and has been suggested as a standard biomarker for the disease (reviewed in Näätänen and Kähkönen, 2009; Light and Swerdlow, 2015).

In chronic schizophrenia, MMN has been associated with cognitive impairment (Baldeweg et al., 2004), Global Assessment of Functioning (GAF) and patients' level of independence (Light and Braff, 2005), social cognition and functioning (Wynn et al., 2010), impaired executive functioning (Toyomaki et al., 2008), and positive symptom scores (Kärgel et al., 2014).

It has not, however, been well-established whether MMN is attenuated in first-episode antipsychotic-naïve schizophrenia (FEANS) patients, let alone first-episode schizophrenia (FES). A recent meta-analysis on 14 studies of MMN in FES concluded that the effect-size of MMN attenuation is small and might be influenced by antipsychotic medication (Haigh et al., 2017). In a recent study from our group we did find attenuated MMN using a dichotic selective attention paradigm in FEANS patients, but no attenuation using a standard MMN paradigm (Oranje et al., 2017).

The reason why MMN attenuation is not found in FES and FEANS patients could be that the neuropathological changes causing MMN attenuation (*e.g.* NMDA-receptor dysfunction (Javitt et al., 1996)) are not yet present at this early stage of the disease or are present only in a subgroup of patients. Alternatively, these changes could be present, but only locally or to a degree too small for the deficits to be measured by the more traditional methods. The activity measured at a single electrode channel (or mean signal across a location-based channel group) sums not just potentials from the nearest underlying cortex but also from potentials generated in many places in cortex. Unfortunately, this is usually ignored in the literature, while studies of the specific, underlying sources of MMN are usually not considered, whether or not they report positive results.

Recently, a method for analysing ERP data based on independent component analysis (ICA) decomposition applied to the continuous (unaveraged) EEG data has been developed and applied to duration deviant MMN modelling and measurement in chronic schizophrenia patients (Makeig et al., 1996; Rissling et al., 2014). By clustering the resulting independent component (IC) processes according to estimated 3-D locations of their equivalent current dipole models (Nunez and Srinivasan, 2006) in a template head model, the effective cortical sources summing to produce scalp ERP features can be identified and evaluated (Makeig et al., 2004; Makeig et al., 2002).

Using this methodology, Rissling et al. (2014) focused on six spatially distinct IC process clusters contributing the most to the MMN and P3a evoked response peaks and showed that these correlated significantly with functional measures including GAF and negative and positive symptom scores in their patient group of medicated chronic schizophrenia patients. They found attenuated duration deviant MMN and P3a amplitudes in four of the six spatial IC clusters and found associations between several functional measures and the amplitude and latency of MMN, P3a and RON (the subsequent 're-orienting negativity' peak in the deviant-standard response difference wave) at the source level, correlations that were not significant using measures of the same difference wave at a frontocentral (Fz to average reference) scalp channel.

We previously reported no MMN or P3a attenuation in a relatively large group of FEANS patients based on scalp recorded amplitudes (Düring et al., 2015). Here we report whether MMN and P3a based on a source-resolved approach provides further insight in this partly the same group of patients. We evaluate frequency-, duration- and combined- (frequency and duration) deviant based MMN and P3a features at the effective source level and correlate them with clinical, cognitive and psychopathological measures. We test whether by using this source-resolved approach we might disentangle the underlying generators of the scalp-recorded MMN and thereby identify subtle changes in a patient group that is antipsychotic-naïve and not (much) influenced yet by disease progress.

2. Materials and methods

2.1. Participants

The data used in this study is part of the Pan European Collaboration Antipsychotic-Naive Studies (PECANS), a large cohort of FEANS patients and matched controls examined with an extensive test battery including cognitive and electrophysiological measures, magnetic resonance imaging and single-photon emission computed tomography. In the current study, baseline data from the cognitive and electrophysiological test battery were analysed. A part of the current sample was previously analysed using a more traditional method and published by Düring and colleagues (Düring et al., 2015). Patients and controls from the same cohort partially overlap with those presented in previous publications on other modalities (Bak et al., 2017; Düring et al., 2015; Düring et al., 2014).

The study was conducted in accordance with the Declaration of Helsinki II and was approved by the Danish National Committee on Biomedical Research Ethics (H-D-2008-088) with clinical trials identifier: NTC01154829. Signed informed consent was provided by all participants.

The total sample of the PECANS study was 69 FEANS patients and 67 healthy controls matched on age, gender and parental socioeconomic status. Of these, 56 FEANS patients and 64 healthy controls had baseline EEG data from the MMN paradigm and were included in this current study. The main reasons for participants' missing baseline

EEG data were related to the need to start treatment or patients withdrawing after initial acceptance. All included patients met the ICD-10 criteria for schizophrenia ($n = 55$) or schizoaffective disorder ($n = 1$). None of the healthy controls had any previous or current mental health issues and no known first-degree relatives with mental health disorders. Neither patients nor healthy controls had participated in psychophysiological studies before. Somatic illness was excluded through physical examination of the patients. Further exclusion criteria were previous impact-related unconsciousness, organic brain damage or disease, substance dependency, known intellectual disability (IQ < 70), diseases or processes contraindicated with amisulpride treatment (*e.g.* allergy, prolactin-producing tumour), as well as involuntarily treatment or treatment under judicial ruling. Substance use was not an exclusion criterion, but its extent and type were noted. Urine samples were collected to screen for benzodiazepine, cannabis, and central stimulant use.

2.2. Clinical, cognitive and psychopathological measures

All participants were tested with a comprehensive neurocognitive test battery including measures from the Cambridge Neuropsychological Test Automated Battery (CANTAB, (Robbins et al., 1994)), the Brief Assessment of Cognition in Schizophrenia (BACS, (Keefe et al., 2004)), the Wechsler Adult Intelligence Scale III (WAIS III, (Wechsler, 1997)), as well as the Danish Adult Reading Test (DART, (Nelson and O'Connell, 1978)). All tests were administered by trained research personnel.

From the extensive number of variables we choose *a priori* to include only cognitive measures similar to those found to be associated with MMN and P3a in the study by Rissling et al. (2014). DART was used to assess premorbid intelligence (similar to the Wide Range Achievement Test (WRAT3)). Number of correct responses from the Digit Sequencing task from the BACS battery was included to mirror the Letter Number Sequencing Test. Number of errors at the extradimensional set shifting stage from the Intra−/Extradimensional Set Shift test (IED) from CANTAB was included to assess perseveration (similar to perseverative errors from the Wisconsin Card Sorting Test (WCST)). The patients' daily function and symptom severity was assessed with the Social and Occupational Functioning Assessment Scale (SOFAS, (Rybarczyk, 2011)) (similar to the Scale of Functioning (SOF, (Rapaport et al., 1996))) and the Global Assessment of Function (GAF, (Hall, 1995)) divided in GAF functional and -social respectively. Severity of symptoms was assessed with the positive and negative syndrome scale (PANSS) interview (Kay et al., 1988) similar to the Scale for the Assessment of Negative and Positive Symptoms (SANS, SAPS, (Andreasen, 1989)).

2.3. EEG processing

The following section is a brief description of the processing. For a full description, see Supplementary Material A – Electrophysiology Methods.All subjects were examined using the Copenhagen Psychophysiological Test Battery (CPTB) (Oranje and Glenthøj, 2014). EEG was recorded with BioSemi hardware (Amsterdam, Netherlands). The paradigm consisted of four stimulus types: Standard tone, Frequency deviant tone, Duration deviant tone and Combined (frequency and duration deviant) tone.

All data processing and analysis was performed in MATLAB R2016b (MATLAB and Statistics Toolbox Release 2016b, The MathWorks, Inc., Natick, Massachusetts, United States) and the MATLAB toolbox EEGLAB (Delorme and Makeig, 2004). For each subject, the raw continuous Biosemi EEG data with associated channel locations was imported re-referenced to average reference, and downsampled to 250 Hz.

A high-pass filter with finite impulse response (FIR) with pass-band edge at 1 Hz (0.5 Hz @-6 dB, filter order 1650), was applied to improve stability of data to facilitate ICA decomposition (Winkler et al., 2015). The data was then semi-automatically cleaned of bad channels and noisy segments using built-in EEGLAB tools.

The preprocessed continuous EEG data was then analysed using Adaptive Mixture Independent Component Analysis (AMICA) (Palmer et al., 2008). After ICA, each dataset had the same number of independent components (ICs) as the rank of the data matrix after channel rejection, giving in total 7489 ICs — 4024 ICs for controls and 3465 ICs for patients (no significant difference between groups, $\chi 2 = 0.033$, $p = 0.86$).

For each IC, the best-fitting equivalent current dipole (ECD) in Talairach space was computed using “DIPFIT” version 2.3, an EEGLAB native plug-in based on FieldTrip (Oostenveld et al., 2011), another open-source software environment for advanced analysis of EEG data. We used a boundary element model (BEM) composed of three 3-D surfaces (skin, skull and cortex) extracted from the Montreal Neurological Institute (MNI) template head model with standard International 10–20 System electrode locations compatible with the Biosemi electrode cap.

Before epoching, a finite impulse response (FIR) filter with pass-band edge at 30 Hz (33.75 Hz @ -6 dB, filter order 110) was applied to remove high-frequency noise.

Each dataset was then epoched according to the four stimulus types from −1 to 2 s relative to stimulus onset. On average, for each subject 1681 epochs were available (SD, 237). Each epoch was baseline-corrected using a reference interval from −100 to 0 ms relative to stimulus onset as baseline.

Finally, the data was cleaned from artefacts using two separate methods: residual variance and clustering (see supplementary methods A for full description).

2.4. Clustering and ERP measures

Equivalent current dipoles (ECDs) for brain-based effective sources ($N = 2387$ ECDs; mean, 19.9 per subject (SD, 6.3); range 5–36) were clustered using K-means clustering based on ECD location in Talairach space. We chose to identify 19 clusters as each subject would then contribute on average one independent component (IC) per cluster, similar to Rissling et al. (2014). One additional cluster contained ICs with outlier ECDs, defined as being further than 3 standard deviations from any of the 19 cluster centroids. This cluster ($N = 79$ ECDs; 59 unique subjects; mean, 0.66 per subject (SD, 0.76); range, 0–3) was excluded from further analysis.

Difference-ERP waveforms were derived for the frequency-, duration- and combined-type deviants: the deviant minus standard response difference for each subject IC and across-subjects IC cluster. Grand-average cluster MMN and P3a measures could then be derived.

Because stimulus onset asynchrony ranged from 300 to 500 ms, we could not, as in Rissling et al. (2014), reliably analyse the re-orienting negativity which occurs at 400 to 600 ms (Schröger and Wolff, 1998).

For subjects having more than one IC in a cluster, we used the mean of these components' ERP waveforms in subsequent analyses of these subjects.

To obtain the latency intervals for measuring MMN and P3a amplitudes and peak latencies, we plotted the whole-sample grand average deviant-standard difference waveform of the data summing all clustered ‘brain’ IC projections to electrode channel FCz for each of the three deviant types (Fig. 1). The scoring intervals were identified as the latencies of the grand average MMN voltage minimum and the P3a voltage maximum +/− 50 ms, similar to other studies (Atkinson et al., 2012; Salisbury et al., 2016). MMN mean amplitude was calculated as mean voltage in the window surrounding the identified peak +/− 20 ms, similar to Rissling et al. (2014).

MMN for the frequency- and combined-type deviants exhibited two negative-going peaks thereby increasing the size of the MMN amplitude measurement window. Each subject's MMN and P3a mean and peak amplitudes and corresponding latencies were selected based on the

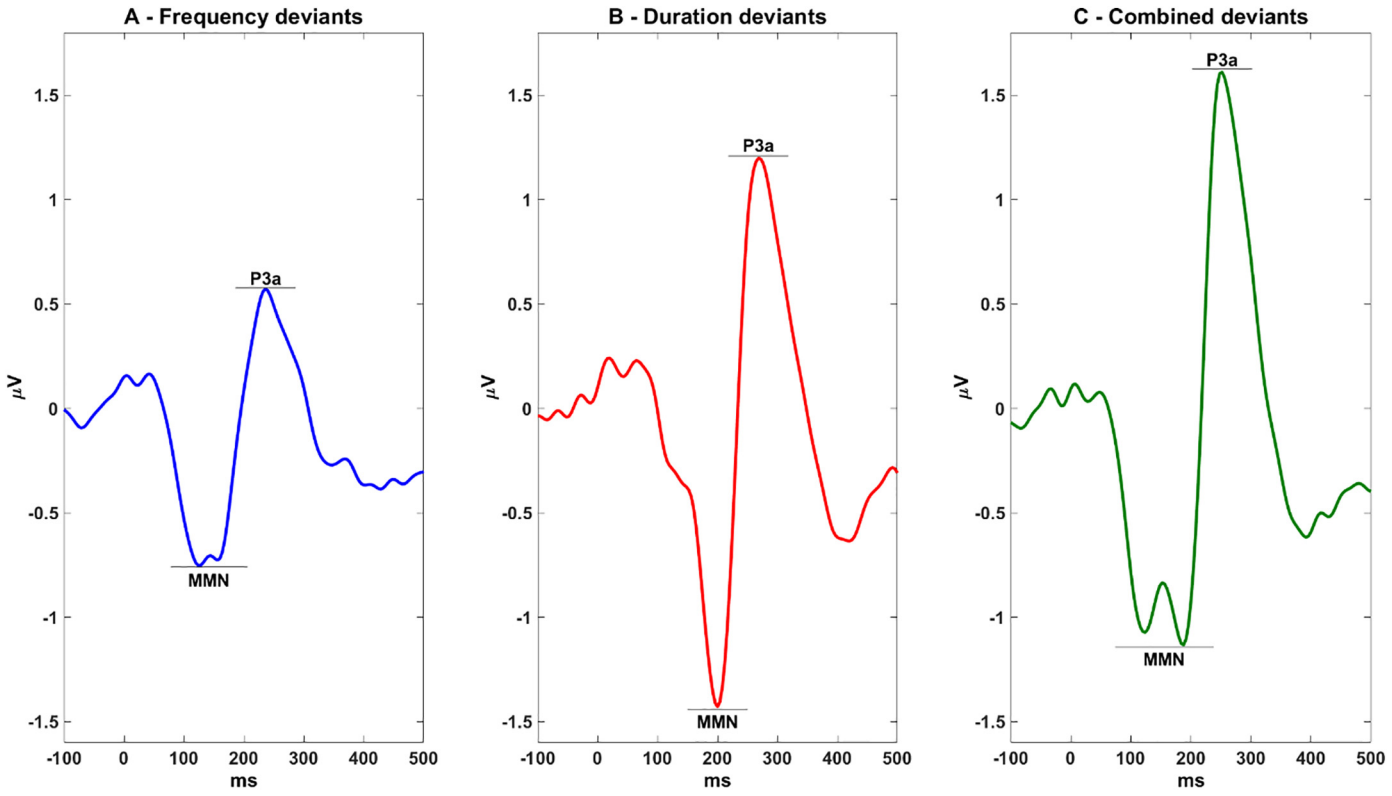

Fig. 1. Whole-sample grand average difference waveform summing all clustered IC projections to electrode channel FCz for each deviant type.

minimum or, for polarity-reversed clusters, maximum peak within the measurement window.

2.5. Statistical analysis

2.5.1. Source location measures

For each cluster, we tested for a significant difference in occupation by FEANS patients and healthy controls using a permutation test where group memberships were permuted randomly 100,000 times. The *p*-value for each cluster was expressed as the proportion of these permutations in which the (permuted) cluster ratio of FEANS patients and healthy controls were equal to or more extreme than the observed ratio.

2.5.2. Response attenuation measures

2.5.2.1. Scalp channel-level measures. To enable comparison of our source-resolved approach with that of the more traditional scalp channel-based method, group differences using the summed 'brain' IC data back-projected to the FCz channel for each of the three deviant types were tested using permutation tests.

2.5.2.2. Source-level measures. The main aim of the current study was to evaluate MMN and P3a attenuation at the cortical source level to search for subtle changes in FEANS patients not usually detectable with the more traditional methods. A previous application of this method found attenuation at six distinct sources for duration deviants in a group of medicated and chronically ill schizophrenia patients (Rissling et al., 2014). Therefore, our *a priori* analysis choices were to test duration deviant MMN and P3a attenuation in these previously identified sources: clusters centred in or near anterior cingulate, dorsal mid-cingulate, medial orbitofrontal, ventral mid-cingulate, R inferior frontal and R superior temporal cortical areas. Group differences for these six clusters were tested for both MMN and P3a peak and mean amplitude using permutation tests. *Post hoc*, any significant findings were then explored in an ANOVA approach to see if the result was influenced by gender or age. Further, the summed 'brain' IC data back-projected to channels corresponding in location to clusters with significant group differences were also tested using permutation tests.

Post hoc the remaining clusters with mean triphasic waveforms exhibiting MMN and P3a peaks at expected latencies were tested for peak and mean amplitude as well as peak latency for all three deviant types. Bonferroni-Holm was used to account for multiple comparisons (270 measures = 15 clusters * 3 – min/max, mean and peak latency * 3 deviants * 2 peaks – MMN and P3a).

2.5.3. Correlation measures

A priori Spearman's non-parametric correlation coefficients were used to test the associations identified by Rissling et al. (2014) between source-level duration MMN and P3a peak and mean amplitude and peak latency and the clinical, cognitive and psychopathological measures. These were: medial orbitofrontal P3a amplitude with SOF, SANS, and SAPS and P3a peak latency with EDS errors; R inferior frontal MMN amplitude with DART and Digit Sequence and MMN and P3a peak latency with EDS errors.

Post hoc Spearman's non-parametric correlation coefficients were used in an exploratory approach to examine the correlation between all ten clinical, cognitive and psychopathological measures and MMN and P3a for all three deviants for all clusters exhibiting triphasic curves as well as the back projected 'traditional' method with MMN and P3a in the relevant latencies (Fig. 2). Bonferroni-Holm was used to account for multiple comparisons (2880 measures = 16 EEG measures (15 clusters + the 'traditional' method) * 10 measures * 3 – min/max, mean and latency * 3 deviants * 2 peaks – MMN and P3a).

3. Results

3.1. Location

Fig. 2 shows whole-sample (patients and controls) cluster grand average IC difference waves for the three deviant types for each of the

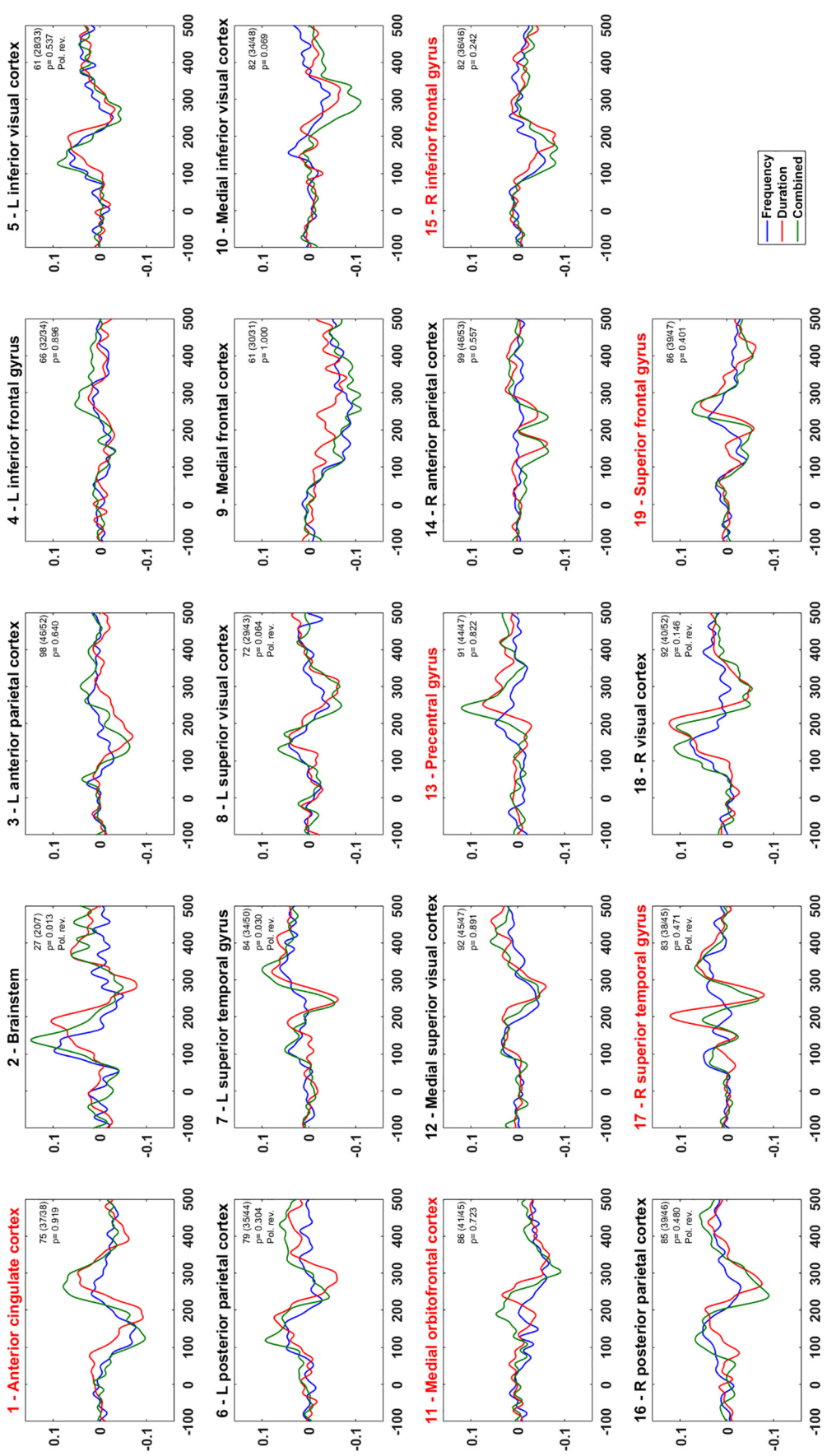

Fig. 2. All-subjects grand average MMN difference waves for each of the three types of deviants (frequency, duration and combined) for each of the 19 clusters. Numbers in top right corners show total number of subjects (FEANS patients/controls) and associated p-values. Pol. rev. = polarity reversed. Red title name indicates the *a priori* chosen clusters. The scale on the vertical axis is IC activation; the magnitude at scalp channels (μV) is obtained by multiplying the IC activation with the inverse of the ICA unmixing matrix.

19 clusters. Sources directly corresponding to those also found by Rissling were: anterior cingulate cortex, medial orbitofrontal cortex, R inferior frontal gyrus and R superior temporal gyrus. One cluster (ventral mid-cingulate cortex) was not found in this study. Another cluster (dorsal mid-cingulate cortex) corresponded to two clusters identified in this study. These two clusters were closer to the cortex; we interpreted their anatomical region as superior frontal gyrus and precentral gyrus. For all three deviants, 9 of the remaining 13 clusters exhibited a triphasic wave with MMN and P3a peaks at expected latencies. Four clusters (medial frontal, medial inferior and superior visual and R anterior parietal cortices) did not show a triphasic waveform. The ratio of contributing FEANS patients to healthy controls was significantly different from random expectation for the cluster at L superior temporal gyrus only ($p = 0.03$), which included fewer FEANS subject (see Fig. 2 for *p*-values).

3.2. Attenuation

3.2.1. Scoring windows

For frequency deviants, MMN and P3a intervals were 78–206 ms and 186–286 ms respectively, for duration deviants, 150–250 ms and 218–318 ms, and for combined-type deviants 74–238 ms and 202–302 ms respectively (Fig. 1).

3.2.2. Scalp channel-level measures

Similar to our previous paper using the more traditional method at electrode FCz and based on part of the current subject population (Düring et al., 2015), we found no group differences in MMN or P3a amplitude measures for any of the three deviants.

Post hoc analysis of channel T8 located outside the cluster at right superior temporal gyrus (see below) revealed no group differences in MMN or P3a amplitude measures for any of the three deviants (Table 1).

3.2.3. Source-level measures

Group comparison of duration deviant MMN and P3a for the six *a priori* chosen clusters revealed significantly smaller MMN peak ($p = 0.03$) and mean ($p = 0.01$) amplitude for FEANS patients compared to controls for the right superior temporal gyrus cluster. Additionally, for the superior frontal gyrus cluster, P3a peak (p = 0.01) but not mean amplitude was significantly smaller in FEANS patients than in controls. These results were not affected by age or gender. None of the other four clusters exhibited significantly different group differences to duration deviants (see also Table 2 and Fig. 3).

Post hoc analysis of the remaining 9 clusters for each of the three deviant types indicated several significant group differences, but none of these survived the Bonferroni-Holm corrections for multiple comparisons (see Supplementary Material B – Additional Data, Table S1).

Table 1
Participants. Group differences were tested by independent two-sample *t*-tests or Chi-Square tests (gender).

	FEANS patients	Healthy controls	p
n	56	64	0.83
Age	24.6 (5.75)	24.8 (5.62)	0.86
Gender (M/F)	31/25	37/27	0.71
DART	21.0 (9.27)	22.9 (6.51)	0.21
Digit Sequence	19.8 (4.64)	22.6 (3.68)	**< 0.001**
EDS errors	10.5 (10.7)	6.15 (7.56)	**0.014**
GAF functional	41.3 (10.8)	–	–
GAF social	40.0 (9.79)	–	–
PANSS total	83.3 (16.3)		
PANSS positive	20.4 (4.22)	–	–
PANSS negative	21.2 (7.30)	–	–
PANSS general	41.8 (8.65)	–	–
SOFAS	42.3 (10.6)	–	–

DART = Danish Adult Reading Test. EDS errors = Errors made at the extra-dimensional shift stage, CANTAB IED Test. Digit Sequence = Number of correct responses, BACS Digit Sequencing Task, PANSS = Positive and Negative Syndrome Scale. GAF = Global assessment of function. SOFAS = Social and occupational functioning assessment scale.
P-values < 0.05 are in bold.

Table 2
P-values for group differences in amplitude measures of duration deviant response differences at the six *a priori* chosen clusters.

Cluster	MMN		P3a	
	Max/Min	Mean	Max/Min	Mean
1 - Anterior cingulate	0.83	0.37	0.51	0.39
11 - Medial orbitofrontal	0.34	0.38	0.36	0.34
13 - Precentral	0.86	0.77	0.18	0.71
14 - R inferior frontal	0.37	0.98	0.97	0.82
17 - R superior temporal	**0.03**	**0.01**	0.26	0.32
19 - Superior frontal	0.18	0.74	**0.01**	0.62

P-values < 0.05 are in bold.

3.3. Correlation

None of the correlations between clinical, cognitive or psychopathological measures with duration deviant MMN and P3a amplitude measures or peak latency reported by Rissling et al. (2014) were found to be significant in the current sample: medial orbitofrontal P3a amplitude with SOFAS ($p = 0.26$), PANSS positive ($p = 0.16$), PANSS negative ($p = 0.35$) and P3a latency with EDS errors ($p = 0.89$); R inferior frontal MMN amplitude with DART ($p = 0.12$) and Digit Sequence ($p = 0.73$) and MMN and P3a latency with EDS errors ($p = 0.24$ and 0.19 respectively).

Post hoc analysis revealed 143 significant correlations for the three deviants, but none of these survived the Bonferroni-Holm corrections for multiple comparisons (see Supplementary Material B – Additional Data, Table S2).

4. Discussion

4.1. General

Here independent component analysis (ICA) was used to evaluate MMN and P3a amplitude measures at the cortical source level in FEANS patients and to correlate these with clinical, cognitive and psychopathological measures. This is to our knowledge the first study on this patient group using this source-resolved approach. Although no group difference in MMN or P3a amplitudes was found at the scalp channel level, the ICA-decomposed data showed significantly attenuated duration deviant MMN in the right superior temporal region as well as significantly attenuated duration deviant P3a amplitude in the superior frontal region in patients compared to healthy controls. No *a priori* defined correlations to behavioural or clinical scores were found to be significant. Further, the *post hoc* correlations between either MMN or P3a at sources with relevant waveforms and the 3 cognitive (DART, Digit Sequence, EDS errors), 3 psychopathological (GAF functional and -social, SOFAS), and 4 clinical measures (PANSS total, −positive, −negative and -general) did not survive corrections for multiple comparisons. Our findings support that MMN and P3a attenuation in schizophrenia are associated with early disease-related changes in supratemporal and frontal brain regions and are not the result of medication or chronicity.

4.2. Cortical source locations

The spatial distribution of the identified sources are in line with previous MMN source localisation studies using other modalities

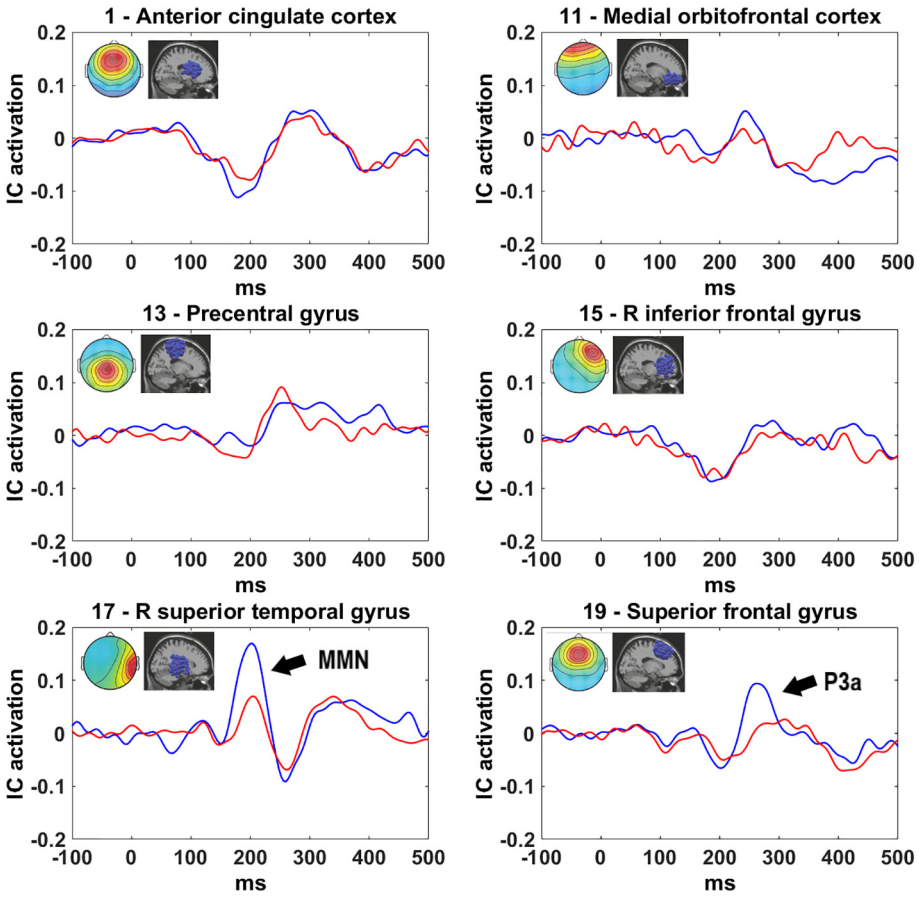

Fig. 3. Duration MMN/P3a waveforms for FEANS patients (red) and controls (blue) for *a priori* chosen clusters. Images in top right corners show cluster-mean projected scalp map (left) and equivalent dipole locations (right). Arrow indicates a significant group difference. Note the positive-going MMN for cluster 17 (R superior temporal), contributing to the MMN positivity at right temporal scalp sites. The scale on the vertical axis is IC activation; the magnitude at scalp channels (μV) is obtained by multiplying the IC activation with the inverse of the ICA unmixing matrix. (For interpretation of the references to color in this figure legend, the reader is referred to the web version of this article.)

(functional magnetic resonance imaging, current source density) indicating contributing sources in bilateral superior temporal gyri, anterior cingulate cortex, and frontal cortical areas (including inferior frontal gyrus) (Gaebler et al., 2015; Kim et al., 2016; Rissling et al., 2014). In our data, triphasic response-difference waveforms in parietal and visual source regions indicate more widespread event-related brain activity during MMN generation. Activity in these regions has also been found in other MMN source-localizing studies (Fulham et al., 2014; MacLean et al., 2015).

An unresolved question is the distribution of subjects within the clusters. While only the cluster in and near left superior temporal gyrus showed a significant difference in group occupancy, not all subjects contributed to each cluster. There could be several reasons for this, such as topological differences in cortical distribution or orientation giving different dipole orientations and locations in different subjects, differences in auditory processing strategies between subjects, or differing numbers of degrees of freedom available for 'brain' ICs because of differences in artefact complexity across subjects. Significantly more ICs were removed as artefactual for patients, likely reflecting the presence of more varied non-brain artefacts in patient data.

4.3. Attenuation

By applying independent component analysis decomposition to EEG data from an MMN paradigm to evaluate MMN and P3a amplitude at a cortical source level, we can for the first time demonstrate that FEANS patients exhibit attenuated duration deviant MMN peak and mean amplitude in the right superior temporal region (containing right auditory cortex) as well as an attenuated duration deviant P3a peak amplitude in the superior frontal region compared to healthy controls.

Our results are in line with other studies reporting attenuated duration- but not frequency deviant MMN peak amplitude in the early stages of schizophrenia (Näätänen and Kähkönen, 2009; Nagai et al., 2013). The finding of attenuated MMN in the auditory cortex is in line with other studies reporting reduced activation of the right (Fulham et al., 2014; Perrin et al., 2017) or left (Solís-Vivanco et al., 2014) auditory cortex in schizophrenia patients during MMN generation.

An attenuated MMN amplitude was not found in FEANS patients relative to controls at our other investigated source regions, indicating that relevant neuropathological changes are subtle or localized to supratemporal and frontal regions at this early stage of the disease, which is consistent with literature (Cobia et al., 2012). The MMN response in the anterior cingulate cortex was not significantly attenuated in our patient group, while it was in chronic schizophrenia patients in the study of Rissling et al. (2014). Whether this progression is due to chronicity, treatment, or increased numbers of psychotic episodes cannot be determined from the data.

There remains hope for developing deviant-tone response differences including MMN into biomarkers for schizophrenia. Our results showing that at least one source of MMN is attenuated (in response to duration deviants) in FEANS patients, as well as one source of the ensuing P3a response difference, adds one more piece to the puzzle. A method for online EEG ICA evaluation has already been established (Pion-Tonachini et al., 2015), potentially enabling future use of this method in the clinic.

4.4. Correlation

The correlations between clinical, cognitive and psychopathological measures and MMN and or P3a measures reported by Rissling et al. (2014) for chronic schizophrenia patients were not replicated for this first-episode antipsychotic-naïve group of patients.

While cognitive deficits have been shown to be stable across the illness (Mesholam-Gately et al., 2009), FEANS patients may have better

global and social functioning than chronic patients. The lack of associations might be explained by smaller variance in MMN and or P3a peak amplitude measures and functional measures compared to chronic schizophrenia patients, possibly due to medication effects or progress of the disease.

While none of our *post hoc* correlations survived Bonferroni-Holm correction for multiple comparisons, several associations were significant before correction (see Supplementary Material B – Additional Data, Table S2). Future studies could test directly the associations found in this study and might also investigate whether, in view of apparent measure dependencies in these data, a more sensitive method of correcting for multiple comparisons might be applicable in further studies.

4.5. Strengths and limitations

The greatest strength of this study is the large sample of FEANS patients. This allowed several thousand equivalent current dipoles, each accounting for a brain effective EEG source found by ICA decomposition of the unaveraged data, to be sorted into large well-defined spatial clusters. While providing high temporal and welcome spatial resolution, the ICA source separation and source clustering methods employed here do not enable us to spatially distinguish auditory cortex and superior temporal gyrus sources. Being able to distinguish between these sources could reveal important mechanics of MMN generation.

It should be mentioned that even though all patients were antipsychotic-naïve, other forms of medication might have influenced our findings.

The preprocessing pipeline used here followed up-to-date recommendations, however, EEG source localization is not ground truth. The brain areas for the identified sources note the centroids of the clusters and should not be seen as a specific point in the brain but rather an area.

ICA and independent source localization and clustering tools are still being improved. The requirement to pre-specify the number of clusters and clustering measures to employ in computing IC-pair distances adds a user-related uncertainty to the method. We clustered on ECD location alone to ensure spatially separable clusters. Including other measures (*e.g.*, ERP, scalp map and power spectrum) could potentially increase the physiological coherence, at the possible cost of spatial coherence.

A standard/deviant tone paradigm taking full advantage of the trial-by-trial analysis approaches made possible by ICA decomposition might give further insights. Although, to our knowledge, such a paradigm has not yet been developed, it could for example involve longer recording sessions, more variegated properties of deviants, and possibly separate sessions for deviant types to better explore the cortical sources active in the auditory deviance response network and their dynamic interrelationships.

5. Conclusion

Our study shows that localized MMN and P3a amplitude attenuation in response differences between average event-related potentials evoked by a nonattended stream of standard and occasional deviant tones, respectively, can be identified in FEANS patients using a source-resolved approach based on identification of sources by independent component analysis. Here, no *a priori* correlations between either MMN or P3a and clinical, cognitive and psychopathological measures were found, and none of the exploratory correlations survived correction for multiple comparisons. Since there is evidence that these associations are present in more chronic populations of schizophrenia patients, this result may indicate that these associations develop gradually in the disease process or are in some part effects of medication.

Conflicts of interest

BG is the leader of a Lundbeck Foundation Center of Excellence for Clinical Intervention and Neuropsychiatric Schizophrenia Research (CINS), which is partially financed by an independent grant from the Lundbeck Foundation based on international review and partially financed by the Mental Health Services in the Capital Region of Denmark, the University of Copenhagen and other foundations. All grants are the property of the Mental Health Services in the Capital Region of Denmark and administrated by them. The remaining authors declare no conflict of interest.

Acknowledgments

This work was supported by the Mental Health Services, The Capital Region, Denmark; and The Lundbeck Foundation (grant number R155-2013-16337). MR received a travel grant from The Lundbeck Foundation (grant number R236-2016-2062). The funders had no role in study design, data collection and analysis, decision to publish, or preparation of the manuscript.

Appendix A. Supplementary data

Supplementary data to this article can be found online at https://doi.org/10.1016/j.nicl.2019.101760.

References

Andreasen, N.C., 1989. The scale for the assessment of negative symptoms (SANS): conceptual and theoretical foundations. Br. J. Psychiatry. Suppl. 49–58.

Atkinson, R.J., Michie, P.T., Schall, U., 2012. Duration mismatch negativity and P3a in first-episode psychosis and individuals at ultra-high risk of psychosis. Biol. Psychiatry 71, 98–104. https://doi.org/10.1016/j.biopsych.2011.08.023.

Bak, N., Ebdrup, B.H., Oranje, B., Fagerlund, B., Jensen, M.H., Düring, S.W., Nielsen, M., GlenthØj, B.Y., Hansen, L.K., 2017. Two subgroups of antipsychotic-naive, first-episode schizophrenia patients identified with a Gaussian mixture model on cognition and electrophysiology. Transl. Psychiatry 7, e1087–e1088. https://doi.org/10.1038/tp.2017.59.

Baldeweg, T., Klugman, A., Gruzelier, J., Hirsch, S.R., 2004. Mismatch negativity potentials and cognitive impairment in schizophrenia. Schizophr. Res. 69, 203–217. https://doi.org/10.1016/j.schres.2003.09.009.

Baumeister, A., Francis, J., 2002. Historical development of the dopamine hypothesis of schizophrenia. J. Hist. Neurosci. 11, 265–277. https://doi.org/10.1076/jhin.11.3.265.10391.

Cobia, D.J., Smith, M.J., Wang, L., Csernansky, J.G., 2012. Longitudinal progression of frontal and temporal lobe changes in schizophrenia. Schizophr. Res. 139, 1–6. https://doi.org/10.1016/j.schres.2012.05.002.

Delorme, A., Makeig, S., 2004. EEGLAB: an open source toolbox for analysis of single-trial EEG dynamics including independent component analysis. J. Neurosci. Methods 134, 9–21. https://doi.org/10.1016/j.jneumeth.2003.10.009.

Doeller, C.F., Opitz, B., Mecklinger, A., Krick, C., Reith, W., Schröger, E., 2003. Prefrontal cortex involvement in preattentive auditory deviance detection: neuroimaging and electrophysiological evidence. Neuroimage 20, 1270–1282. https://doi.org/10.1016/S1053-8119(03)00389-6.

Düring, S., Glenthøj, B.Y., Andersen, G.S., Oranje, B., 2014. Effects of dopamine D2/D3 blockade on human sensory and sensorimotor gating in initially antipsychotic-Naïve, first-episode schizophrenia patients. Neuropsychopharmacology 3000–3008. https://doi.org/10.1038/npp.2014.152.

Düring, S., Glenthøj, B.Y., Oranje, B., 2015. Effects of blocking D2/D3 receptors on mismatch negativity and P3a amplitude of initially antipsychotic na??, first episode schizophrenia patients. Int. J. Neuropsychopharmacol. 19, 1–7. https://doi.org/10.1093/ijnp/pyv109.

Escera, C., Alho, K., Winkler, I., Näätänen, R., 1998. Neural mechanisms of involuntary attention to acoustic novelty and change. J. Cogn. Neurosci. 10, 590–604. https://doi.org/10.1162/089892998562997.

Friston, K., Brown, H.R., Siemerkus, J., Stephan, K.E., 2016. The dysconnection hypothesis (2016). Schizophr. Res. https://doi.org/10.1016/j.schres.2016.07.014.

Fulham, W.R., Michie, P.T., Ward, P.B., Rasser, P.E., Todd, J., Johnston, P.J., Thompson, P.M., Schall, U., 2014. Mismatch negativity in recent-onset and chronic schizophrenia: a current source density analysis. PLoS One. https://doi.org/10.1371/journal.pone.0100221.

Gaebler, A.J., Mathiak, K., Koten, J.W., König, A.A., Koush, Y., Weyer, D., Depner, C., Matentzoglu, S., Edgar, J.C., Willmes, K., Zvyagintsev, M., 2015. Auditory mismatch impairments are characterized by core neural dysfunctions in schizophrenia. Brain. https://doi.org/10.1093/brain/awv049.

Garrido, M.I., Kilner, J.M., Kiebel, S.J., Friston, K.J., 2007a. Evoked brain responses are generated by feedback loops. Proc. Natl. Acad. Sci. U. S. A. 104, 20961–20966.

https://doi.org/10.1073/pnas.0706274105.
Garrido, M.I., Kilner, J.M., Kiebel, S.J., Stephan, K.E., Friston, K.J., 2007b. Dynamic causal modelling of evoked potentials: a reproducibility study. Neuroimage 36, 571–580.
Giard, M.H., Perrin, F., Pernier, J., Bouchet, P., 1990. Brain generators implicated in the processing of auditory stimulus deviance: a topographic event-related potential study. Psychophysiology 27, 627–640. https://doi.org/10.1111/j.1469-8986.1990.tb03184.x.
Haigh, S.M., Coffman, B.A., Salisbury, D.F., 2017. Mismatch negativity in first-episode schizophrenia: a meta-analysis. Clin. EEG Neurosci. 48, 3–10. https://doi.org/10.1177/1550059416645980.
Hall, R.C.W., 1995. Global assessment of functioning. Psychosomatics 36, 267–275. https://doi.org/10.1016/S0033-3182(95)71666-8.
Javitt, D.C., Steinschneider, M., Schroeder, C.E., Arezzo, J.C., 1996. Role of cortical N-methyl-D-aspartate receptors in auditory sensory memory and mismatch negativity generation: implications for schizophrenia. Proc. Natl. Acad. Sci. U. S. A. 93, 11962–11967. https://doi.org/10.1073/pnas.93.21.11962.
Javitt, D.C., Zukin, S.R., Heresco-Levy, U., Umbricht, D., 2012. Has an angel shown the way? Etiological and therapeutic implications of the PCP/NMDA model of schizophrenia. Schizophr. Bull. 38, 958–966. https://doi.org/10.1093/schbul/sbs069.
Kärgel, C., Sartory, G., Kariofillis, D., Wiltfang, J., Müller, B.W., 2014. Mismatch negativity latency and cognitive function in schizophrenia. PLoS One 9. https://doi.org/10.1371/journal.pone.0084536.
Kay, S.R., Opler, L.A., Lindenmayer, J.P., 1988. Reliability and validity of the positive and negative syndrome scale for schizophrenics. Psychiatry Res. 23, 99–110. https://doi.org/10.1016/0165-1781(88)90038-8.
Keefe, R.S.E., Goldberg, T.E., Harvey, P.D., Gold, J.M., Poe, M.P., Coughenour, L., 2004. The brief assessment of cognition in schizophrenia: reliability, sensitivity, and comparison with a standard neurocognitive battery. Schizophr. Res. 68, 283–297. https://doi.org/10.1016/j.schres.2003.09.011.
Kim, M., Ik Kevin Cho, K., Bryan Yoon, Y., Young Lee, T., Soo Kwon, J., 2016. Aberrant Temporal Behavior of Mismatch Negativity Generators in Schizophrenia Patients and Subjects at Clinical High Risk for Psychosis. https://doi.org/10.1016/j.clinph.2016.11.027.
Lieder, F., Stephan, K.E., Daunizeau, J., Garrido, M.I., Friston, K.J., 2013. A Neurocomputational model of the mismatch negativity. PLoS Comput. Biol. 9. https://doi.org/10.1371/journal.pcbi.1003288.
Light, G., Braff, D., 2005. MIsmatch negativity deficits are associated with poor functioning in schizophrenia patients. Arch. Gen. Psychiatry 62, 127–136.
Light, G., Swerdlow, N., 2015. Future clinical uses of neurophysiological biomarkers to predict and monitor treatment response for schizophrenia. Ann. N. Y. Acad. Sci. 1344, 105–119. https://doi.org/10.1111/nyas.12730.
MacLean, Shannon E., Blundon, Elizabeth G., Ward, Lawrence M., 2015. Brain regional networks active during the mismatch negativity vary with paradigm. Neuropsychologia 75, 242–251.
Makeig, S., Bell, J., Jung, T.-P., Sejnowski, T.J., 1996. Independent component analysis of electroencephalographic data. Adv. Neural Inf. Proces. Syst. 145–151. https://doi.org/10.1109/ICOSP.2002.1180091.
Makeig, S., Westerfield, M., Jung, T.P., Enghoff, S., Townsend, J., Courchesne, E., Sejnowski, T.J., 2002. Dynamic brain sources of visual evoked responses. Science 295, 690–694. https://doi.org/10.1126/science.1066168.
Makeig, S., Delorme, A., Westerfield, M., Jung, T., Townsend, J., Courchesne, E., Sejnowski, T.J., 2004. Electroencephalographic brain dynamics following visual targets requiring manual responses. Science 2, 1–29 (80-.).
Mesholam-Gately, R.I., Giuliano, A.J., Goff, K.P., Faraone, S.V., Seidman, L.J., 2009. Neurocognition in first-episode schizophrenia: a meta-analytic review. Neuropsychology 23, 315–336. https://doi.org/10.1037/a0014708.
Näätänen, R., Kähkönen, S., 2009. Central auditory dysfunction in schizophrenia as revealed by the mismatch negativity (MMN) and its magnetic equivalent MMNm: a review. Int. J. Neuropsychopharmacol. 12, 125–135. https://doi.org/10.1017/S1461145708009322.
Näätänen, R., Paavilainen, P., Rinne, T., Alho, K., 2007. The mismatch negativity (MMN) in basic research of central auditory processing: a review. Clin. Neurophysiol. 118, 2544–2590. https://doi.org/10.1016/j.clinph.2007.04.026.
Nagai, T., Tada, M., Kirihara, K., Yahata, N., Hashimoto, R., Araki, T., Kasai, K., 2013. Auditory mismatch negativity and P3a in response to duration and frequency changes in the early stages of psychosis. Schizophr. Res. 150, 547–554. https://doi.org/10.1016/j.schres.2013.08.005.
Nelson, H., O'Connell, A., 1978. Dementia: the estimantion of premorbid intelligence levels using the new adult Reading test. Cortex 14, 234–244. https://doi.org/10.1016/S0010-9452(78)80049-5.
Nunez, P.L., Srinivasan, R., 2006. Electric Fields of the Brain: The Neurophysics of EEG: Medicine & Health Science Books, 2nd edition. Oxford University Press, Oxford.
Olney, J.W., Newcomer, J.W., Farber, N.B., 1999. NMDA receptor hypofunction model of schizophrenia. J. Psychiatr. Res. https://doi.org/10.1016/S0022-3956(99)00029-1.
Oostenveld, R., Fries, P., Maris, E., Schoffelen, J.M., 2011. FieldTrip: open source software for advanced analysis of MEG, EEG, and invasive electrophysiological data. Comput. Intell. Neurosci. 2011, 156869. https://doi.org/10.1155/2011/156869.
Opitz, B., Rinne, T., Mecklinger, A., von Cramon, D.Y., Schröger, E., Yves Von Cramon, D., Schröger, E., 2002. Differential contribution of frontal and temporal cortices to auditory change detection: fMRI and ERP results. Neuroimage 15, 167–174. https://doi.org/10.1006/nimg.2001.0970.
Oranje, B., Glenthøj, B.Y., 2014. Clonidine normalizes levels of P50 gating in patients with schizophrenia on stable medication. Schizophr. Bull. 40, 1022–1029. https://doi.org/10.1093/schbul/sbt144.
Oranje, B., Aggernaes, B., Rasmussen, H., Ebdrup, B.H., Glenthøj, B.Y., 2017. Selective attention and mismatch negativity in antipsychotic-naïve, first-episode schizophrenia patients before and after 6 months of antipsychotic monotherapy. Psychol. Med. 47, 2155–2165. https://doi.org/10.1017/S0033291717000599.
Palmer, J., Makeig, S., Kreutz-Delgado, K., Rao, B.D., 2008. Newton method for the ICA mixture model. In: ICASSP, IEEE Int. Conf. Acoust. Speech Signal Process. - Proc, pp. 1805–1808. https://doi.org/10.1109/ICASSP.2008.4517982.
Perrin, M.A., Kantrowitz, J.T., Silipo, G., Dias, E., Jabado, O., Javitt, D.C., 2017. Mismatch negativity (MMN) to spatial deviants and behavioral spatial discrimination ability in the etiology of auditory verbal hallucinations and thought disorder in schizophrenia. Schizophr. Res. https://doi.org/10.1016/j.schres.2017.05.012.
Pion-Tonachini, L., Hsu, S.H., Makeig, S., Jung, T.P., Cauwenberghs, G., 2015. Real-time EEG source-mapping toolbox (REST): online ICA and source localization. Proc. Annu. Int. Conf. IEEE Eng. Med. Biol. Soc. EMBS. https://doi.org/10.1109/EMBC.2015.7319299.
Powers, A.R., Mathys, C., Corlett, P.R., 2017. Pavlovian conditioning–induced hallucinations result from overweighting of perceptual priors. Science 357 (80-.).
Rapaport, M.H., Bazzetta, J., McAdams, L.A., Patterson, T., Jeste, D.V., 1996. Validation of the scale of functioning in older outpatients with schizophrenia. Am. J. Geriatr. Psychiatry 4, 218–228. https://doi.org/10.1097/00019442-199622430-00005.
Rinne, T., Alho, K., Ilmoniemi, R.J., Virtanen, J., Näätänen, R., 2000. Separate time behaviors of the temporal and frontal mismatch negativity sources. Neuroimage 12, 14–19. https://doi.org/10.1006/nimg.2000.0591.
Rissling, A.J., Miyakoshi, M., Sugar, C.A., Braff, D.L., Makeig, S., Light, G.A., 2014. Cortical substrates and functional correlates of auditory deviance processing deficits in schizophrenia. NeuroImage Clin. 6, 424–437. https://doi.org/10.1016/j.nicl.2014.09.006.
Robbins, T.W., James, M., Owen, A.M., Sahakian, B.J., McInnes, L., Rabbit, P., 1994. Cambridge neuropsychological battery (CANTAB): a factor analytic study of a large sample of normal elderly volunteers. Dement. Geriatr. Cogn. Disord. 5, 266–281.
Rybarczyk, B., 2011. Social and occupational functioning assessment scale (SOFAS). In: Encyclopedia of Clinical Neuropsychology. Springer New York, New York, NY, pp. 2313. https://doi.org/10.1007/978-0-387-79948-3_428.
Salisbury, D.F., Polizzotto, N.R., Nestor, P.G., Haigh, S.M., Koehler, J., McCarley, R.W., 2016. Pitch and duration mismatch negativity and premorbid intellect in the first hospitalized schizophrenia Spectrum. Schizophr. Bull. 43, sbw074. https://doi.org/10.1093/schbul/sbw074.
Schröger, E., Wolff, C., 1998. Attentional orienting and reorienting is indicated by human event-related brain potentials. Neuroreport 9, 3355–3358.
Shelley, A.M., Ward, P.B., Catts, S.V., Michie, P.T., Andrews, S., McConaghy, N., 1991. Mismatch negativity: an index of a preattentive processing deficit in schizophrenia. Biol. Psychiatry 30, 1059–1062. https://doi.org/10.1016/0006-3223(91)90126-7.
Solís-Vivanco, R., Mondrag-Maya, A., Len-Ortiz, P., Rodrguez-Agudelo, Y., Cadenhead, K.S., de la Fuente-Sandoval, C., 2014. Mismatch negativity reduction in the left cortical regions in first-episode psychosis and in individuals at ultra high-risk for psychosis. Schizophr. Res. 158, 58–63. https://doi.org/10.1016/j.schres.2014.07.009.
Toyomaki, A., Kusumi, I., Matsuyama, T., Kako, Y., Ito, K., Koyama, T., 2008. Tone duration mismatch negativity deficits predict impairment of executive function in schizophrenia. Prog. Neuro-Psychopharmacol. Biol. Psychiatry 32, 95–99. https://doi.org/10.1016/j.pnpbp.2007.07.020.
Waberski, T.D., Kreitschmann-Andermahr, I., Kawohl, W., Darvas, F., Ryang, Y., Gobbelé, R., Buchner, H., 2001. Spatio-temporal source imaging reveals subcomponents of the human auditory mismatch negativity in the cingulum and right inferior temporal gyrus. Neurosci. Lett. 308, 107–110.
Wacongne, C., Changeux, J.-P., Dehaene, S., 2012. A neuronal model of predictive coding accounting for the mismatch negativity. J. Neurosci. 32, 3665–3678. https://doi.org/10.1523/JNEUROSCI.5003-11.2012.
Wechsler, D., 1997. WAIS-III: Wechsler adult intelligence scale. In: Administration and Scoring Manual, third ed. Psychological Corporation, San Antonio, TX.
Winkler, I., 2007. Interpreting the mismatch negativity. J. Psychophysiol. 21, 147–163. https://doi.org/10.1027/0269-8803.21.34.147.
Winkler, I., Debener, S., Muller, K.R., Tangermann, M., 2015. On the influence of high-pass filtering on ICA-based artifact reduction in EEG-ERP. Proc. Annu. Int. Conf. IEEE Eng. Med. Biol. Soc. EMBS 2015–Novem 4101–4105. https://doi.org/10.1109/EMBC.2015.7319296.
Wynn, J.K., Sugar, C., Horan, W.P., Kern, R., Green, M.F., 2010. Mismatch negativity, social cognition, and functioning in schizophrenia patients. Biol. Psychiatry 67, 940–947. https://doi.org/10.1016/j.biopsych.2009.11.024.